## POLITECNICO DI TORINO
## Repository ISTITUZIONALE

New 3d segmentation approach for reverse engineering selective sampling acquisition

*Availability:*
This version is available at: 11583/1835350 since:

*Publisher:*

*Published*
DOI:10.1007/s00170-006-0772-3

*Terms of use:*

*Publisher copyright*

(Article begins on next page)

19 May 2024

*NEW 3D SEGMENTATION APPROACH FOR REVERSE ENGINEERING SELECTIVE SAMPLING*
*ACQUISITION*

**A. Courtial, E. Vezzetti**

*Dipartimento di Sistemi di Produzione Ed Economia dell'Azienda, Politecnico di Torino, Corso Duca degli*
*Abruzzi 24, 10129,Torino, Italy*
*Tel.: +39 011 5647294; Fax: +39 011 5647299; e-mail: enrico.vezzetti@polito.it*

**Abstract**

The "Segmentation", i.e. the three dimensional point clouds partition in different morphological zones, is a necessary operation while approaching the reverse engineering cycle, because it helps the operator in generating the surface model. This operation is usually developed after the acquisition and the pre-processing phases, and it tries to define a boundary grid which the following surface fitting operation will employ for the surface model definition. Many approaches apply the segmentation methods far from the 3D scanner device. On the contrary, this research work proposes an iterative strategy which starts from a first raw point acquisition, then it partitions the object surface and identifies the boundary of those zones showing significant morphological features (shape-changes). As a consequence, they will be re-digitised with deeper scansions, in order to reach a more precise morphological information. This partitioning operation is driven by a morphology descriptor, the Guassian Curvature, giving and estimation of the local surface morphological complexity. Moreover the proposed algorithm employs the 3D scanner measuring uncertainty to define a "curvature variation threshold", in order to identify those zones showing significant morphological shape-changes.

**Keywords:** Reverse Engineering, Scanning Strategy, Geometric Morphology

## 1. Introduction

Reverse Engineering process generates a virtual representation of an existing part, based on point data acquisition by employing several measuring techniques. The first acquired point data generally requires pre-processing operations such as noise filtering and smoothing, in order to give a well structured point cloud to the subsequent virtual model reconstruction operations.

3D Scanning devices usually acquire the object surface by using a constant pitch which is a compromise among the highest resolution reachable by the measuring system, the virtual model requested accuracy and the acquisition time. Sometimes the use of laser (non contact) devices [1] represents the best solution giving good results in term of acquisition speed and point density, but it is affected by some limitations for what concerns measurement accuracy. The best solution is often the use of CMMs (contact devices), which perform high accuracy but need long acquisition time, if high resolution is required [2]. On the other hand, when the application needs high accuracy in short time, or it works with wide surfaces, both contact and non-contact solutions seem to be inappropriate.

Actually, this problem is usually solved by dividing the process in two steps: in the first one, the operator develops a preliminary object acquisition of the object surface, in a second time, he/she "decides" which zones need a deeper scansions looking at the first acquired model (mesh). This operation is long time consuming, strongly subjective and depends on the experience of the acquisition developer [3]. As considering the importance of this operation, in term of Reverse Engineering times and costs, it is necessary to give it a more structured and objective behaviour, in order to obtain an automated algorithm performing what the 3D scanner operator manually does.
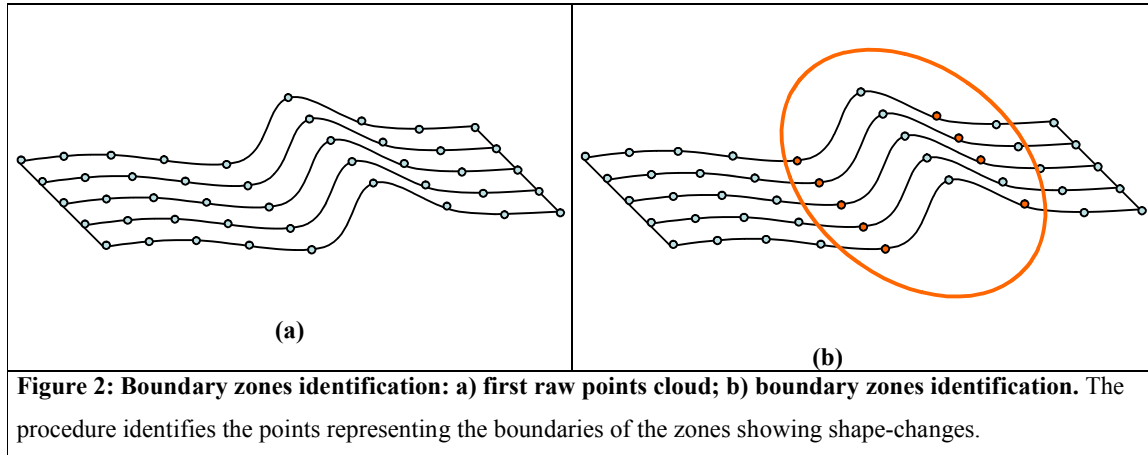
## 2. Approach description

The solution proposed in this paper starts thinking that every object is characterised by multi-patches surfaces. This means that an object surface is a collection of geometries with different morphological complexity levels (planes, cylinder, cones, …).  On the basis of this hypothesis it is impossible to think about applying the same acquisition pitch on all the surfaces, considering that we move in range that starts from a linear formalisation, as in a planar surface till arriving to quadratic, cubic and so on, covering the scenario of all three-dimensional geometries [4] (Fig.1).



**Figure 1: An example of object surface composed by different morphological complexities features**
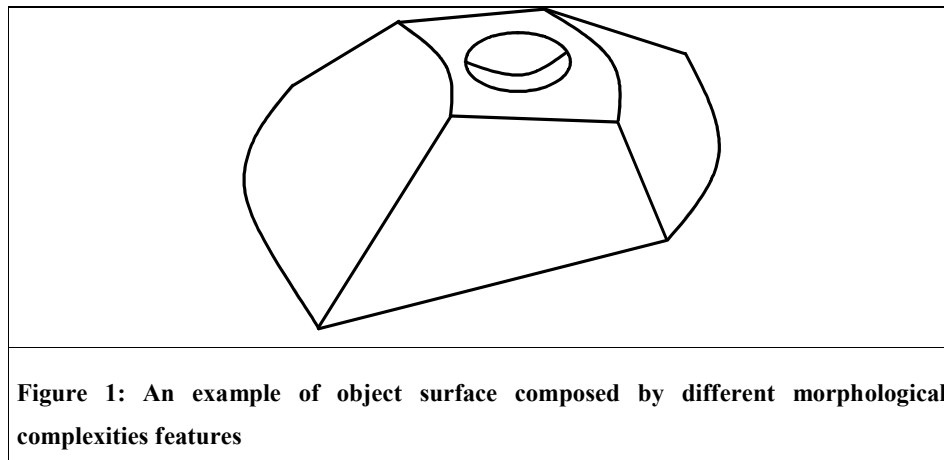
As a consequence of this consideration, it is necessary to develop a procedure able to divide the points cloud into different morphological zones, by the identification of their boundaries. This is strongly relevant to define the best acquisition pitch for the different surface formalisations (describing different object surface partitions), in relation with the morphology complexity level of the different features composing the object surface.

These operations need an intrinsic geometrical parameter to be selected, able to describe the global complexity of the digitised surface, working on shape-change detection (Fig.2). The points cloud dividing operation is oriented to the surface boundary definition, and it's already implemented during the Reverse Engineering cycle, under the name of "Segmentation". In fact, it is usually applied after pre-processing steps, and has to divide the points cloud in zones, in order to prepare the acquired data for the following curve/surface fitting operation. Previous researches utilized two basically different approaches to partition measurement point data: namely "edge-based" and "face-based" methods, even if there are also some hybrid methods [5,6]. The edge-based method works by trying to find boundaries in the point data representing edges between surfaces. If edges are being sought, an edge-linking process follows, in which disjoint edge points are connected to form

continuous edges. This technique thus infers the surfaces from the implicit segmentation provided by the edge curves.



**Figure 2: Boundary zones identification: a) first raw points cloud; b) boundary zones identification.** The procedure identifies the points representing the boundaries of the zones showing shape-changes.

The second technique or 'face-based' method goes in the opposite direction, and tries to infer connected regions of points with similar properties as groups of points belonging to the same surface. Then edges are derived from the surfaces, by other computations. The hybrid methods usually perform different combinations between the two techniques already pointed out.

While usually the segmentation step goes before the surface fitting one and the 3D surface model building, in the proposed approach the segmentation procedure has also an important role in the acquisition phase (Fig.3). In fact, the segmentation step has to be developed after the first raw acquisition, in order to divide a surface object in zones needing a deeper scansion, and zones needing no more acquisitions, in relation with a local morphological complexity evaluation. The procedure works on a shape-change methodology, and identifies the boundaries of the different morphological zones characterizing the entire surface.
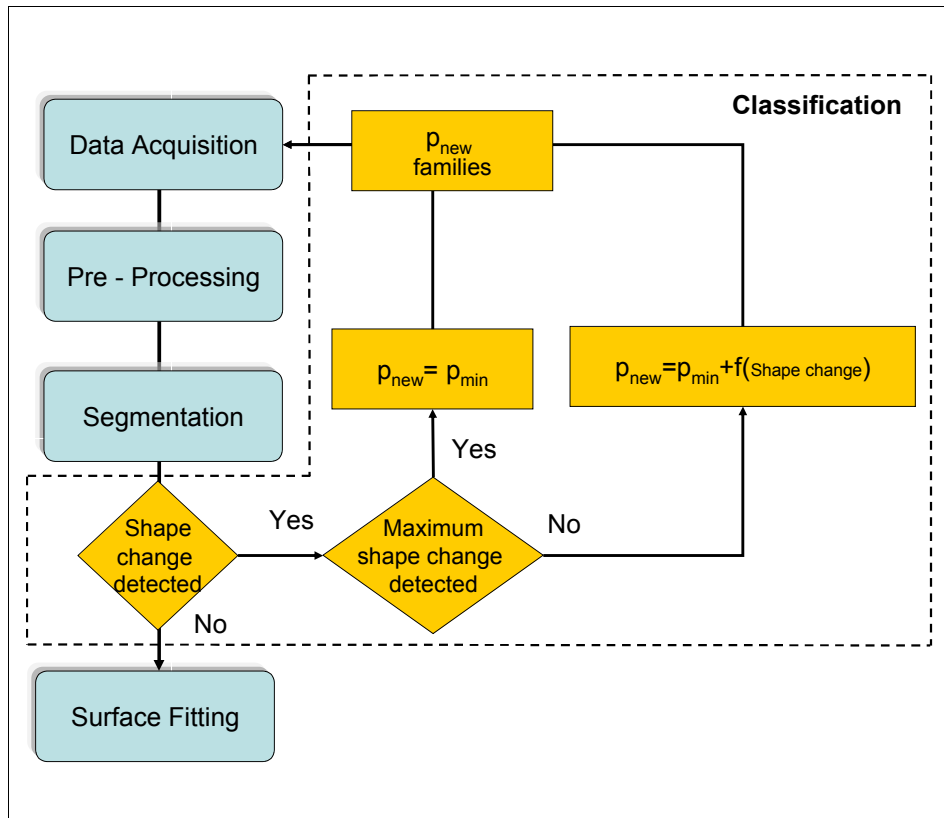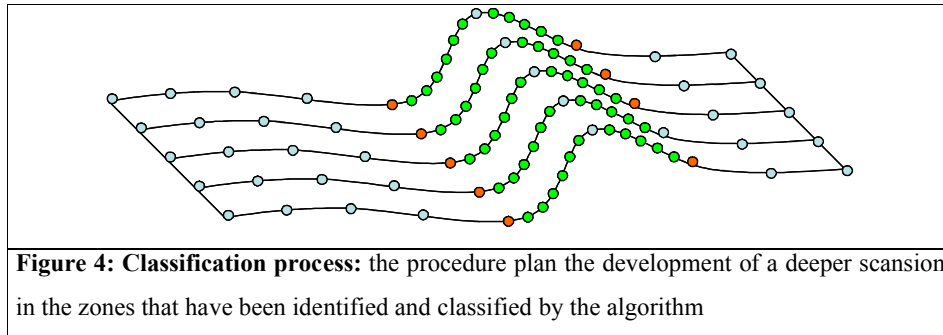
**Figure 3: Proposed Reverse Engineering Cycle:** the segmentation step has to be developed after the first raw acquisition, in order to divide a surface object in zones needing a deeper scansion, and zones needing no more acquisitions, in relation with a local morphological complexity evaluation. If the shape change is detected it is necessary to evaluate the new deeper scansion pitch $p_{new}$. if the maximum value of shape change is identified $p_{new}$ is set to the minimum pitch reachable by the 3D scanner otherwise it will be a function of the shape change identified.
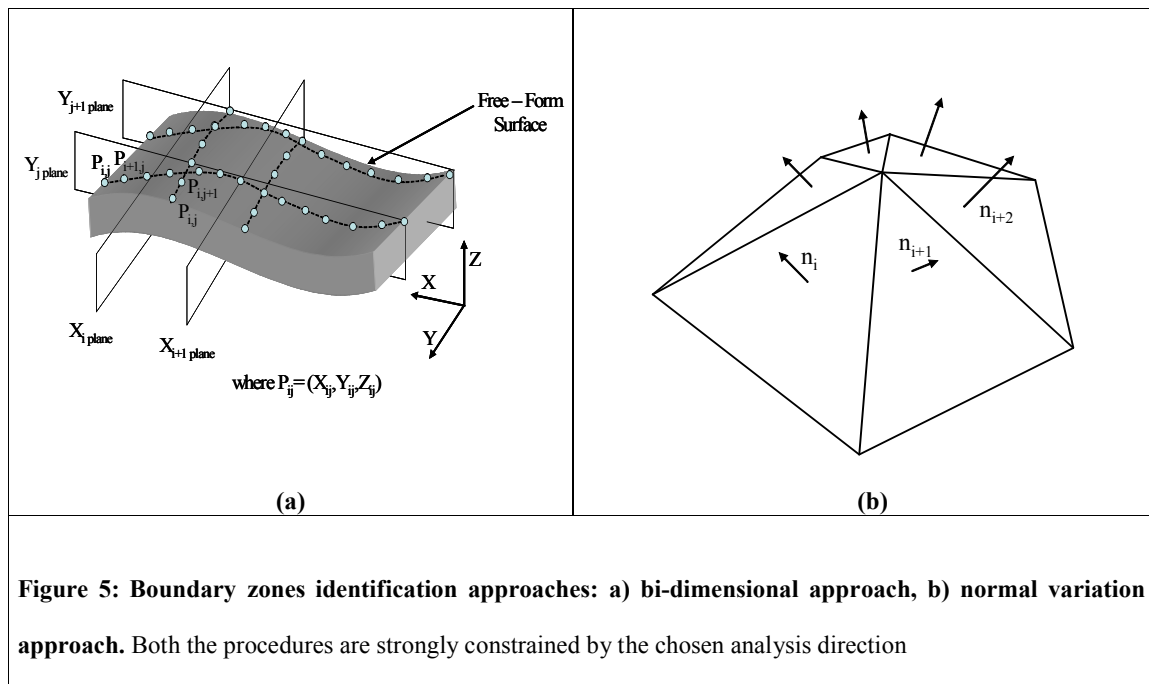
Furthermore, the shape-change detection has to be implemented on a surface approximation given by a points cloud, which was obtained as output of a measuring device (3D Scanner). So the procedure applies the concept of measuring system uncertainty, which will be better explained in the following paragraphs, in order to define a reliable threshold for the shape-change detection process. The classification phase follows the segmentation one: it "classifies" the identified zones in relation to the new acquisition pitch, which was decided in proportion to the identified complexity. This means that the classification methodology, in this approach, will sometimes increase the number of points, where the points cloud shows lack of information but, on the other hand, it will be also able to decrease this number where the first raw points cloud is already too dense in proportion to the identified morphological complexity, and so it brings redundant information. At the moment the algorithm differentiate the identified zones only into two families: those needing a deeper scansion (the procedure will develop a new acquisition inside their boundaries, which were identified in the previous acquisition), and those which will remain completely untouched (fig.4).

**Figure 4: Classification process:** the procedure plan the development of a deeper scansion in the zones that have been identified and classified by the algorithm

## 2.1 Point cloud management

It is actually necessary to find a geometrical parameter able to give an efficient estimation of the local morphological complexity of the object surface working on points cloud. Looking at literature, it is possible to find experience made working with estimation of normal vectors behaviour[7]. These methods show good results but impose a specific direction analysis, as some bi-dimensional approach [8,9].

In fact, the approach which works by dividing the points cloud by parallel planes to the 3D Scanner working frame (X-Y) (Fig.5a), or which considers the normal vector variation behaviour along a specific direction (Fig.5b), gives only the information related to the chosen specific direction. If the object is characterised by shape-changes along other directions from $x$ and $y$ axes, these previous methods will not be able to catch them.



**(a)**                                              **(b)**

**Figure 5: Boundary zones identification approaches: a) bi-dimensional approach, b) normal variation approach.** Both the procedures are strongly constrained by the chosen analysis direction
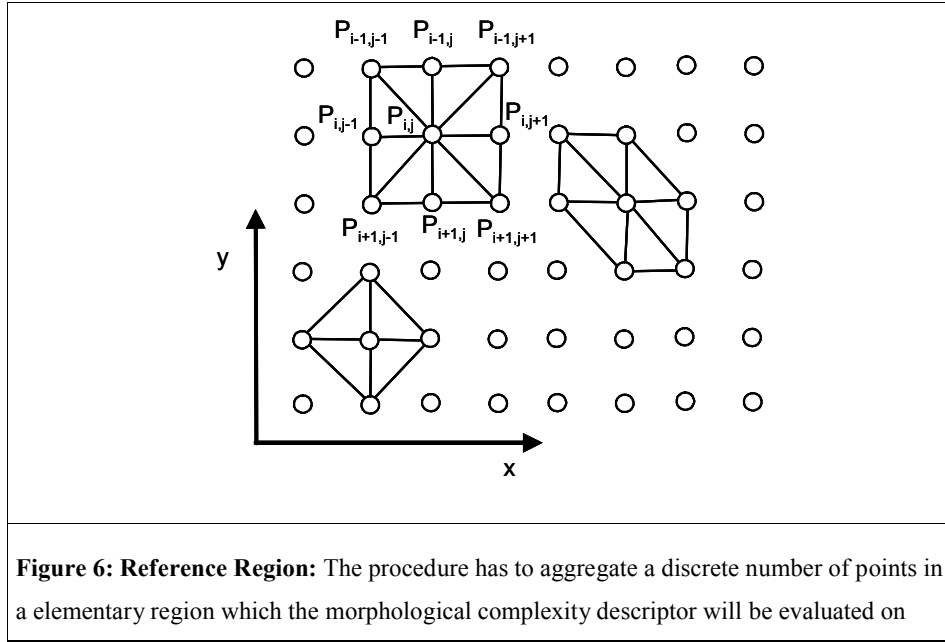
In order to improve the method proposed in the previous paper and to find a solution to the directional problem, the research work has been moved to another approach, based on a morphological parameter disjoined from the normal vectors evaluation. On the other hand, the parameter was directly linked to the points composing the points cloud. Starting from the hypothesis to work on structured grids, and only on internal points (in the following lines they will be called "nodes"), the proposed method associates to every "node", called $\mathbf{P}_{i,j}$, an intrinsic information about the local morphological complexity $M_{i,j}$.

$$\mathbf{P}_{i,j} \text{ and } M_{i,j} \qquad i \in [2:n-2] \qquad j \in [2:m-2] \tag{1}$$

Where $n$ is the number of points along the $x$-axis and $m$ is the number of points along the $y$-axis, while the indexes $i$ and $j$ represent the position of the *nodes* inside the points cloud.
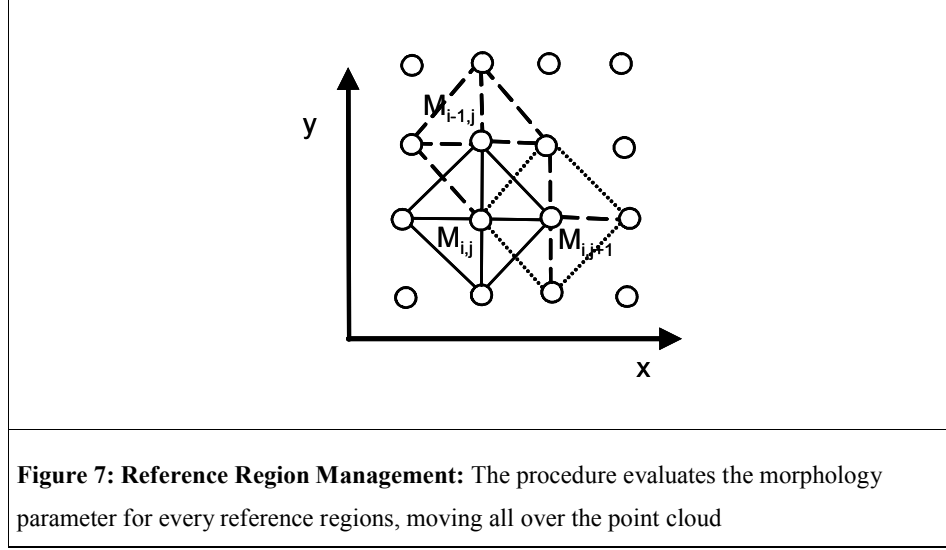
In order to extrapolate this morphological information about the node neighbourhood it is necessary to work with the node surrounding points, creating a "**Reference Region**", that will be characterised by a specific value of the morphological descriptor. It is possible to obtain different reference region configurations by varying the region shape and the number of the aggregated surrounding points (Fig.6).



**Figure 6: Reference Region:** The procedure has to aggregate a discrete number of points in a elementary region which the morphological complexity descriptor will be evaluated on

Beyond the reference region dimension and shape, the algorithm moves all around the point cloud nodes, and creates a complete description of the local surface morphology (morphological map):

$$\mathbf{M} = \begin{bmatrix} M_{i,j} & M_{i,j+1} & \cdots \\ M_{i+1,j} & \cdots & \cdots \\ \cdots & \cdots & M_{n-2,m-2} \end{bmatrix} \tag{2}$$

All the elements of the **M**-matrix will be evaluated by creating the reference region around each point of the cloud. The evaluation process will be characterised by a partial reference region overlapping (Fig.7).

**Figure 7: Reference Region Management:** The procedure evaluates the morphology parameter for every reference regions, moving all over the point cloud

This procedure gives a complete morphological description of the entire object surface. In this way the directionality problem which affected previous cited methods (normal vector variation evaluation, parallel planes method), is completely solved thanks to a complete complexity map of the surface. In fact, it is possible to start from a random node and know how the morphological parameter behave, while moving towards every surrounding nodes.

## 2.2 Morphological descriptor: Gaussian Curvature

The necessity to have an intrinsic and global parameter, able to give a complete description of the entire object surface but also to grant a local description of the morphological complexity, led to employ the Gaussian Curvature [10]. Starting from some concepts about differential surfaces, it is possible to define the Total Curvature $T$ as the integral of the Gaussian Curvature $K$, extended to a finite surface domain $A^*$ [11].

$$T = \int_{A^*} KdA \tag{3}$$

Moreover, the Gauss-Bonnet formula[12] can be used in order to prove that the same formalisation applied to differentiable geometry, is also extensible to a triangulated one, modifying the original equation in the following one:

$$K = 2\pi - \sum_{i=1}^{n} \vartheta_i \tag{4}$$

This new formalisation means that the Gaussian curvature, equivalent to the total curvature on a neighbourhood composed by triangular faces sharing a central node, is the node angular excess. In fact it is the difference between the limit condition of $2\pi$ and the sum of the angles that converge in the node, evaluated on every faces (Fig.8).
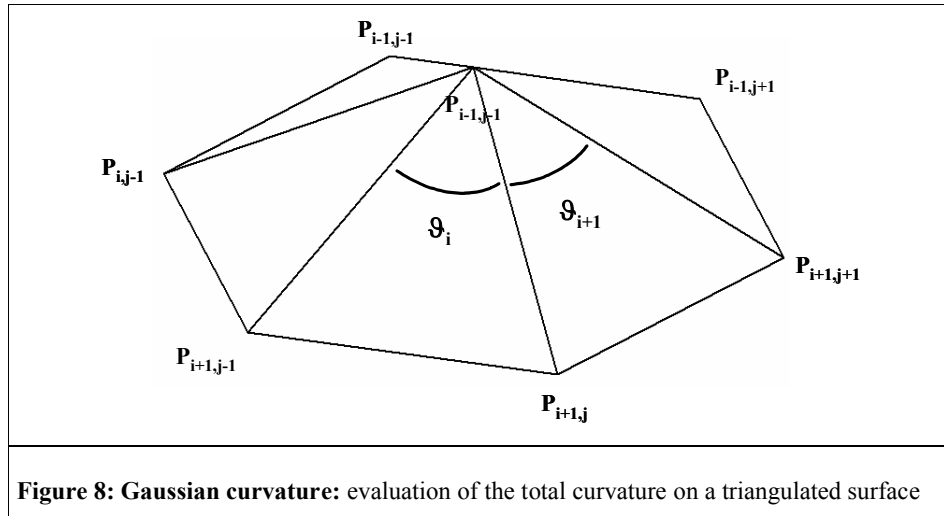
**Figure 8: Gaussian curvature:** evaluation of the total curvature on a triangulated surface

If we work with a triangulated planar surface, the Gaussian curvature will be zero as could be simply verified considering that the convergent angles to the node for a planar surface is $2\pi$. These considerations can easily be extended to other geometries as cylinders or cones, assuming not to consider particular conditions, as for instance those neighbourhoods containing the cone vertex [13,14]. So the **M**-matrix which collects the morphological descriptors $M_{i,j}$ and was described in the previous paragraph, come to be equal to a **K**-matrix collecting the Gaussian Curvature $K_{i,j}$ for every node $\mathbf{P}_{i,j}$.

## 2.3 Boundary definition

Once defined the morphological descriptor it is possible to decide the optimal dimension and geometry of the reference region. Looking at the possible combinations the best choice has seemed to be six triangles, so an hexagonal configuration. In this way it is possible to describe geometries with different curvature types: spherical, hyperbolical, and complex hyperbolical (Fig.9). In particular the last possible configuration, the complex hyperbolical, is particularly suitable for locally describing Free-form surfaces, usually found when a reverse engineering system is employed.

**Figure 9: Reference region configuration:** the use of six vertexes can locally describe geometries with different curvature types: a) spherical; b) hyperbolical; c) complex hyperbolical
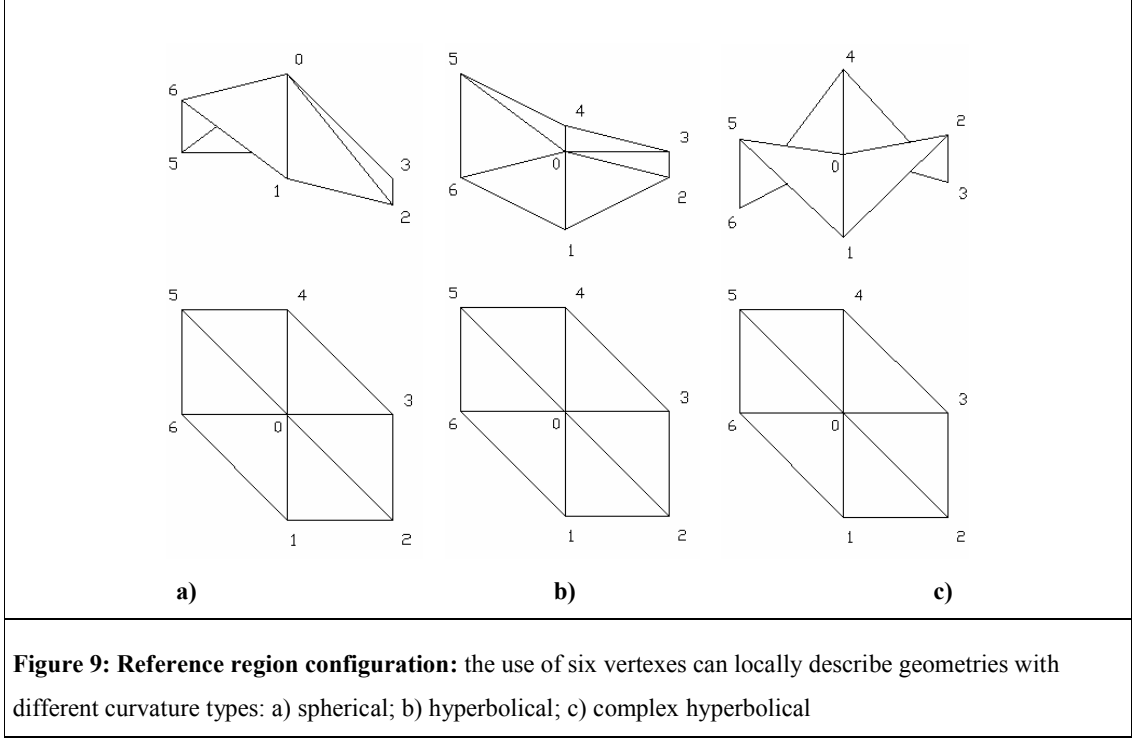
The number of triangles converging to the central node of each reference region has been fixed to six. The scalar product definition can simplify the Gaussian Curvature Formula in term of relative coordinates to the central node.

$$K = 2\pi - \sum_{i=1}^{6} \vartheta_{i,i+1} \tag{5}$$

$$K = 2\pi - \sum_{i=1}^{6} \arccos\left\{ \frac{(x_i - x_0)(x_{i+1} - x_0) + (y_i - y_0)(y_{i+1} - y_0) + (z_i - z_0)(z_{i+1} - z_0)}{\sqrt{(x_i - x_0)^2 + (y_i - y_0)^2 + (z_i - z_0)^2} \sqrt{(x_{i+1} - x_0)^2 + (y_{i+1} - y_0)^2 + (z_{i+1} - z_0)^2}} \right\} \tag{6}$$

where the central node of the geometry is called $P_0$ and the boundary vertexes are indexed with numbers from 1 to 7 assuming $P_1 = P_7$. This means that the Gaussian Curvature formalisation introduces twenty-one variables, because it considers all the points coordinates of the reference region.

Once decided the morphological parameter and the dimension and geometry of the reference region it is necessary to evaluate the variation of the Gaussian curvature. A threshold value has to be defined in order to do so, and it must be able to filter all the eventual noise introduced by the 3D Scanner during the digitisation phase, and then to select only those points presenting significant shape-changes. So the 3D Scanner Uncertainty must be introduced in the threshold evaluation. So the extended uncertainty $U$ of the Gaussian Curvature $K$ has to be used in order to obtain this information for the shape-change detection.

Every introduced variable gives an uncertainty component generated by the 3D scanner performances contributing to the $K$ uncertainty. As a consequence we should consider the following matrix:

$$[\mathbf{u}^2(\xi)] = \begin{bmatrix} u^2(\xi_1) & \bullet & u(\xi_1,\xi_m) & \bullet & u(\xi_1,\xi_{21}) \\ \bullet & \bullet & \bullet & \bullet & \bullet \\ u(\xi_l,\xi_1) & \bullet & u^2(\xi_l) & \bullet & u(\xi_l,\xi_{21}) \\ \bullet & \bullet & \bullet & \bullet & \bullet \\ u(\xi_{21},\xi_1) & \bullet & u(\xi_{21},\xi_m) & \bullet & u^2(\xi_{21}) \end{bmatrix}_{21X21} \tag{7}$$

containing all the variances and co-variances related with every coordinates variable $\xi = x \vee y \vee z$.

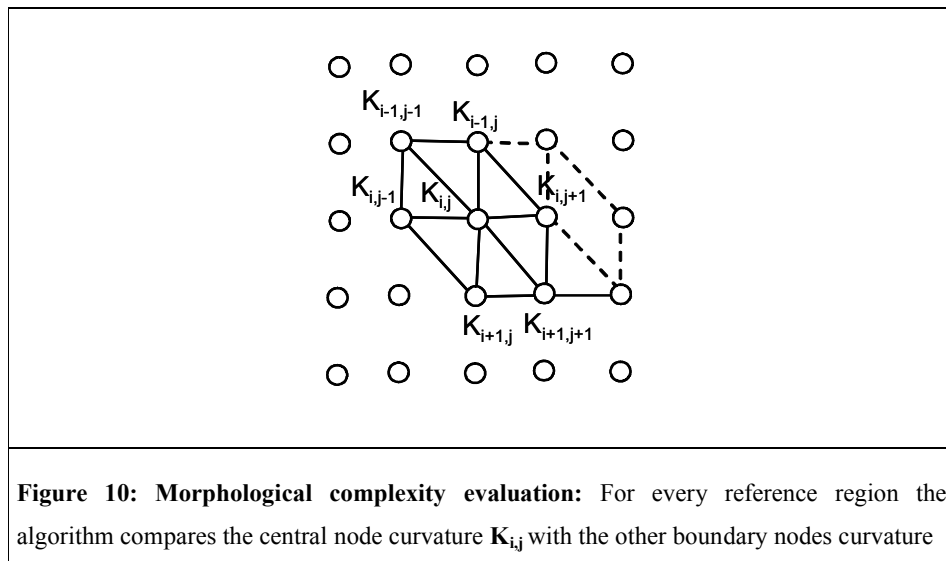The influence of every points coordinates could be evaluated calculating the sensibility coefficients $c_j = \left(\dfrac{\partial K}{\partial \xi_j}\right)$ that could be organised in the following vector:

$$\{\mathbf{C}\} = \left\{ \left(\frac{\partial K}{\partial \xi_1}\right) \quad , \quad \left(\frac{\partial K}{\partial \xi_m}\right) \quad , \quad \left(\frac{\partial K}{\partial \xi_{21}}\right) \right\}_{21X1}^{T} = \{c_1 \quad , \quad c_m \quad , \quad c_{21}\}_{21X1}^{T} \tag{8}$$

We introduce now a *t* factor *(covering factor)* depending on the statistical distribution type employed for qualify the noise affecting the point coordinate variables. This factor enter the following formula for the extended uncertainty evaluation:

$$U(K) = t \cdot \sqrt{\{\mathbf{C}\}_{1X21}^{T}[\mathbf{s}^2(\xi)]_{21X21}\{\mathbf{C}\}_{21X1}} \tag{9}$$

In order to evaluate the curvature variation the strategy followed by the algorithm implements a comparison inside the reference region, comparing the central node curvature $K_{i,j}$ with those of the boundary points ($K_{i-1,j-1}$ $K_{i-1,j}$ $K_{i,j+1}$ $K_{i,j-1}$ $K_{i+1,j}$ $K_{i+1,j+1}$). This procedure detects if there is a significant shape-change surrounding the specific node analysed (Fig.10).



**Figure 10: Morphological complexity evaluation:** For every reference region the algorithm compares the central node curvature $\mathbf{K_{i,j}}$ with the other boundary nodes curvature

If the absolute value of the biggest curvature variation $K_{i,j}$ of the evaluated reference region is over the

extended uncertainty computed $U(K_{i,j})$ this means that the reference zone need a deeper scansion and so the central node is stored.

$$\left|K_{i,j} - K_{l,m}\right| \geq U(K_{i,j}) \qquad \text{where} \quad l = (i-1),(i+1); \quad m = (j-1),(j+1) \qquad (10)$$

This operation is developed for all the reference zones, collecting only those showing a curvature value over the statistical threshold. Once developed a complete map of the points cloud the algorithm will define the different region collecting all the nodes selected during the previous phases.

## 3. Experimental validation

In a first phase, the method has been tested using an ideal geometry. The acquisition process has been simulated by generating a set of measurement points on a known surfaces (characterized by a significant curvature variation). Then a random (Gaussian) perturbation has been added to the coordinate values of the acquired surface points, in order to simulate the variability due to the measurement uncertainty and evaluate the sensitivity of the method in terms of the measuring uncertainty and the surface morphology.

A revolution surface with a sinusoidal generator formalisation has been created in order to understand how the algorithm solves the directionality problems evidenced by previous methods. The perturbation amplitude on the geometry shape has been imposed with the same amount of the real measuring device uncertainty ($u_{cost} = 0.025$ mm) (Fig.11).

$$z = A \cdot \sin\left(\frac{\sqrt{x^2 + y^2}}{T}\right) \qquad (10)$$
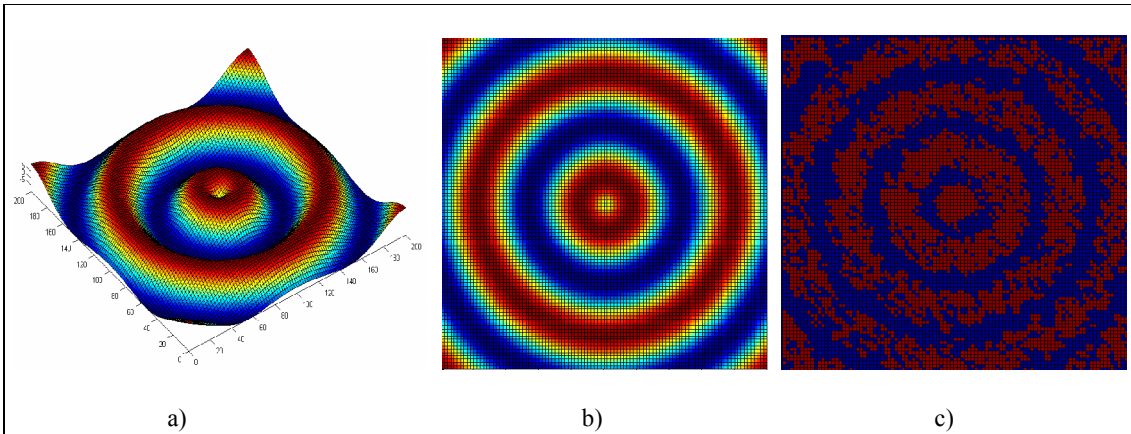


a)          b)          c)

**Figure 11: Surface for the sensitivity test: a, b) points cloud obtained in a simulated acquisition on an ideal noised surface with given curvature variations, c) (red poin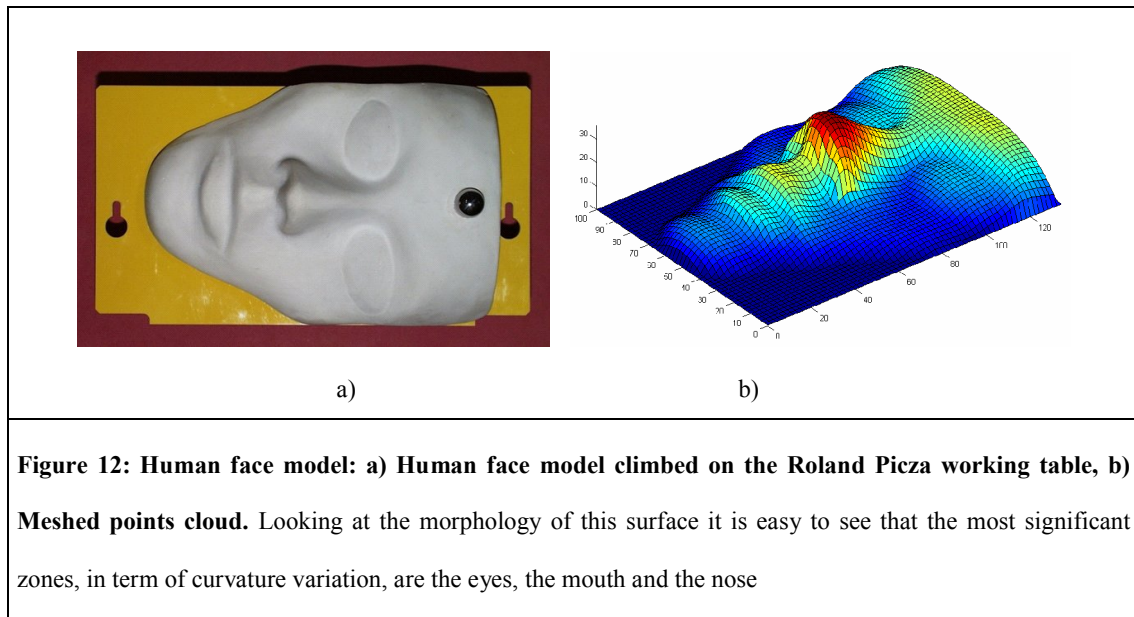ts) zones that need a deeper scansion. All the points belonging to the zones identified for the deeper scansion are coloured in red, in order to facilitate visualisation instead of showing only the region boundaries.**
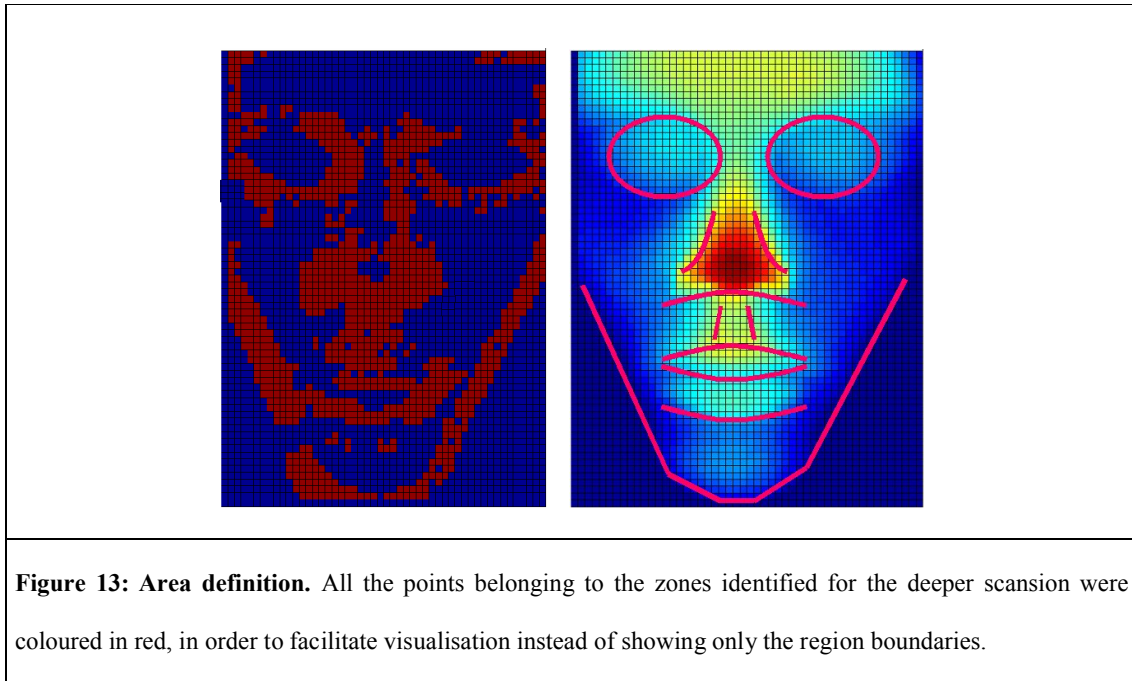
As it is possible to see in figure 12, the algorithm caught circumferential zones, and it is coherent with the geometry behaviour. This underlines the ability of the method to detect shape-changes over 360°, thus solving the directionality constraint which affected the previous methods [8,9,10]. In a second phase of this study a real object surface has been digitised by using the Roland Picza contact 3D Scanner, in order to complete the experimental validation of the procedure.

This acquisition device employs a piezoelectric sensor for the digitisation process. The system is composed by a head, and a working table. The head has a piezoelectric sensor connected with a small needle able to move outside of the head, along the $z$ axis direction, in order to touch the scanned surface. The head is also climbed on a guide allowing another freedom degree along the $x$ direction. The last movement is given to the working table, which translates along the $y$ direction.

The positioning system has a maximum resolution value of 0,05 mm along $x$ and $y$ axis, for the grid acquisition. We decided to test the new algorithm on the same human face (Fig.12a) employed with previous works [9,10], in order to maintain a certain coherence and a consistent comparison with those approaches. Looking at the morphology of this surface (Fig. 12b) it is easy to see that the most significant zones, in term of curvature variation, are the eyes, the mouth and the nose. The other regions of the object do not show any significant morphological variations and can be considered as constant-curvature zones.

A first raw digitisation of the surface was performed using a 2 mm x 2 mm scanning pitch. Looking at the results (Fig.13), it is possible to see a good level of coherence among the expected regions and the individuated zones with significant curvature variations.



a)                                          b)

**Figure 12: Human face model: a) Human face model climbed on the Roland Picza working table, b) Meshed points cloud.** Looking at the morphology of this surface it is easy to see that the most significant zones, in term of curvature variation, are the eyes, the mouth and the nose

**Figure 13: Area definition.** All the points belonging to the zones identified for the deeper scansion were coloured in red, in order to facilitate visualisation instead of showing only the region boundaries.

## 4. Conclusions

The paper describes an automatic procedure for selective identification of sampling points in reverse engineering applications. Its aim is to individuate the boundaries of curvature variation zones, which need further scansions. The methodology is based on the curvature analysis of sampled surfaces. The discrimination between zones with different curvature variations is carried out by using the metrological characteristics of the inspection device. In particular, a threshold value for the difference curvature variation values has been developed on the basis of the inspection device measurement uncertainty.

The methodology has been applied to different kind of free-form patterns. Looking at the obtained results, it is possible to say that this procedure has a good level of applicability in automated scansion systems. The use of scanning device measurement uncertainty turns out a general purpose procedure for identification of critical zones without the operator involvement.

The sensibility of the method depends on the first scanning pitch dimension, on the measurement system uncertainty and on the smoothness of the tested surface.

Even if other approaches developed in previous research works gave good results, the new proposed one maintains a good coherence with the surface morphology but is completely disjoined from any specific analysis direction. In fact, working with the *reference region* concept linked with the Gaussian curvature parameter means having a complete description of the local complexity of every surfaces.

The attention focused on the acquisition phase of the Reverse Engineering process is mainly justified by the necessity of relying on efficient object digitisations in order grant the development of consistent mathematical model reconstruction processes. Far from the 3D scanner, every pre-processing or segmentation strategies could help the CAD operator in the 3D surface model reconstruction, but could also create artificial noise altering the real shape of the object. For this reason it is necessary, when manually managing the object in the acquisition phases, first to use the right 3D scanner and also having the possibility to define the right pitch for the geometrical features to acquire.

In fact, the next step in our research activity is moving in the direction of creating a more fine classification process that will try to identify the right scanning tool (3D Scanner) in relation with morphological characteristics of the object, and also the deeper scansion pitch related to the complexity of the different surface zones: in other words, to improve the 3D scanner performances.

## 5. References

1. Varady T, Martin RR, Cox J. Reverse engineering of geometric models—an introduction. Computer-Aided-Design 1997;29(4):255–268

2. Tornincasa S., Vezzetti E., "Feasibility study of a reverse engineering system benchmarking", Proceedings of ADM-Ingegraf, June 2005, Siviglia Spagna.

3. K. Kase, A. Makinouchi, T. Nakagawa, H Suzuki, F. Kimura, Shape error evaluation method of free-form surfaces, Computer Aided Design 1999, 31; 495-505

4. T. Varady, P. Benko, Reverse engineering B-rep models from multiple point. in Proceedings of Geometric Modeling and Processing, April 2000, IEEE, Hong Kong, pp. 3–12.

5. Sarkar B, Menq C-H. Smooth-surface approximation and reverse engineering. Computer-Aided Design 1991;23(9):623–628

6. Sarkar B, Menq C-H. Smooth-surface approximation and reverse engineering. Computer-Aided Design 1991;23(9):623–628

7. Motavalli S, Bidanda B. Modular software development for digitizingsystems data anaylsis in reverse engineering applications: case of concentric rotational part. Computers and Industrial Engineering 1994;26(2):395–410.

8. H. Woo, E. Kang, Semyung Wang, Kwan H. Lee, A new segmentation method for point cloud data, International Journal of Machine Tool & Manufacture, 42 (2002) 167–178

9. Vezzetti E., Reverse engineering: a selective sampling acquisition approach, International Journal of Advanced Manufacturing Technology (article in press)

10. Galetto M., Vezzetti E.,  Reverse engineering of free-form surfaces: a methodology for threshold definition in selective sampling, International Journal of Machine Tool & Manufacture, (article in press)

11. W.Sun C. Bradley, Y.F.Zhang, H.T.Loh, Cloud data modelling employing a unified, non redundant triangular mesh, Computer Aided Design 33, pp.183 – 193, 2001

12. Fava F., Fondamenti di Geometria Differenziale, Libreria editrice universitaria Levrotto e Bella, Torino, 1991

13. Hoffman R, Jain AK. Segmentation and classification of range images. IEEE Transactions on Pattern Analysis and Machine Intelligence 1987;PAMI-9(5):608–620.

14. J.M.Sullivan, Curvature measures for discrete surfaces, University of Illinois, IL61801, October 2002